

## AN EXPERIMENTAL INVESTIGATION OF STATOR CLOCKING EFFECTS IN A TWO-STAGE LOW-SPEED AXIAL COMPRESSOR

J. Städing\*, D. Wulff, G. Kosyna

Pfleiderer-Institut, TU Braunschweig  
38106 Braunschweig, Germany

Email: staeding@pfi.tu-bs.de, d.wulff@tu-bs.de,  
g.kosyna@tu-bs.de

B. Becker, V. Gümmel

Rolls-Royce Deutschland Ltd & Co KG  
15827 Blankenfelde-Mahlow, Germany

Email: bernd.becker@rolls-royce.com,  
volker.guemmer@rolls-royce.com

### ABSTRACT

The impact of stator clocking on performance and flow of a 2.5-stage axial compressor has been investigated. Stator clocking, the circumferential indexing of adjacent stator rows with equal blade counts, is known as a potential means to modify the flow field in multistage turbomachinery and increase overall efficiencies of both turbines and compressors. These potential effects on turbomachine performance are due to wake-airfoil interactions and primarily depend on the alignment of the downstream stator row with the upstream stator wake path. The present survey describes and discusses the experimental research on stator clocking effects in a low-speed 2.5-stage axial flow compressor, using front loaded CDA blade sections and cantilevered stator rows with identical blade counts. Conventional static pressure tappings were used to locate global peaks in compressor performance for varying Stator 2 clocking positions at different flow coefficients. Results of unsteady total pressure measurements obtained by means of a high-frequency pressure transducer, embedded in the Stator 2 leading edge, give information on Stator 1 wake propagation. Traverse data from pneumatic 5-hole probes show the impact of stator indexing on Stator 2 exit total pressure at different blade spans. Regardless of flow coefficient, the variations of overall compressor efficiency due to Stator 2 clocking are around 0.2% and are exhibiting a near-sinusoidal trend over the clocking angle. It is shown that total pressure measurements at mid-span of Stator 2 leading edge suggest best overall performances for design and low loading conditions, if the Stator 1

wakes pass through mid-passage of Stator 2. At high loading, however, maximum efficiency locates the wake path directly at the leading edge. Due to a considerable span-wise skewness of the upstream stator wake, the aerodynamic clocking position for Stator 2 varies from hub to tip. While it is shown again that this effect weakens the advantages of airfoil indexing on a global scale, stator clocking shows much more potential if only a single blade section is considered.

### NOMENCLATURE

$D$	Diameter
$h/H$	Fractional channel height
$j$	Number of measurement cycles
$l$	Chord length
$M$	Torque
$\dot{m}$	Stage inlet massflow rate
$n$	Rotational speed
$p$	Static pressure
$Q$	Dynamic pressure
$r, \Theta, z$	Compressor polar coordinate system
$s$	Tip clearance
$T$	Static temperature
$W_z$	Axial flow velocity
$x, y, z$	Compressor cartesian coordinate system
$Y$	Specific work
$z$	Number of rotor blade passings
$\beta$	Absolute flow angle
$\gamma$	Isentropic coefficient

\*Adress all correspondence to this author.

$\Delta$	Differential value
$\zeta$	Loss coefficient
$\eta$	Efficiency
$\Theta$	Position stator pitch
$\nu$	Hub to tip ratio
$\Pi$	Pressure ratio
$\varphi$	Flow coefficient
$\psi$	Pressure coefficient
$\bar{p}_t$	Time-averaged total pressure
$\bar{p}_t(t)$	Ensemble-averaged total pressure
$\langle p_t \rangle$	Pitch-averaged total pressure

## Subscripts

0,1,2,3,4,5	Measuring planes
C	Casing
D	Design point conditions
i	Inner specific work
max	maximum efficiency
mean	arithmetic mean of measurements
min	minimum efficiency
ms	mid-span
REF	Reference clocking position
t	Total conditions
tt	Total-to-total
S2	Stator 2
ss	Static-to-static

## Abbreviations

<i>CDA</i>	Controlled diffusion airfoil
<i>CLP</i>	Clocking position
<i>ISA</i>	International standard atmosphere
<i>LSRC</i>	Low-speed research compressor
<i>TTL</i>	Transistor-transistor logic

## INTRODUCTION

The crucial objective of compressor research is to realize a higher pressure rise in less stages while further increasing the already advanced level of overall efficiency. For this purpose the necessity for profound understanding of the complex multistage flow physics and a higher modelling fidelity increases. Clocking is one method to influence the flow field in multistage turbomachinery by changing the relative circumferential positions of either adjacent rotor or stator rows preferably with the same blade count. Not only does clocking present a convenient means to improve compressor efficiency without requiring additional equipment, a systematic investigation of the clocking effect will also expand our knowledge on wake-airfoil interactions and encourage their consideration in the design process.

Even though the majority of research on this topic has been conducted in turbines, a decent number of experimental and numerical studies on the aerodynamic influence of airfoil clocking in compressors has been published. One of the few experimental investigations on stator clocking and its potential to increase efficiency in a low-speed environment was performed by Barankiewicz & Hathaway [1] in a four-stage axial compressor. The changes due to vane indexing were 0.2% in overall compressor performance and 5% to 10% in Stator 3 total pressure loss coefficient, depending on operating condition. For the peak efficiency operating condition, optimum global performance occurred, when the upstream stator wake passed through mid-passage of Stator 3. At higher loading, however, the clocking position, that caused wake impingement on the leading edge, turned out to be the most beneficial. Opposite findings on the effect of upstream wake impingement were reported by Key et al. [2, 3] who investigated the vane indexing effect in a 3-stage medium-speed axial compressor. The results promised a second stage efficiency variation of 0.27% for design load and 1.07% for high loading. In addition, a frequency analysis of the flow field fluctuations was performed, showing that the interaction between the upstream vane wake and the boundary layer of the downstream vane strongly depends on the indexing configuration. Experimental surveys on clocking accompanied by numerical efforts were conducted by Huang et al. [4] and Saren et al. [5] with similar results concerning the clocking position for highest efficiency and variations in compressor performance reaching from 0.5% to 1%. Further investigations on multistage flow physics have shown that the aerodynamic effects of stator clocking are sensitive to the axial spacing between blade rows (Layachi & Bölcs [6], Huang et al. [7] and Saren et al. [5]) and transonic flow environments will react differently to a circumferential shift in upstream wakes as compared to subsonic flows (He et al. [8]). Walker et al. [9] and Solomon et al. [10] investigated the periodic transition on the outlet stator row of a 1.5-stage low-speed compressor with respect to different blade loadings and IGV clocking positions. It was verified that the periodicity of boundary layer transition was strongly influenced by both parameters. Furthermore, the skewness of the upstream IGV wake led to different unsteady flow characteristics from hub to tip. A detailed research on the clocking effect in a 1.5-stage turbine by König et al. [11, 12] names three main factors that influence the alteration of the total pressure loss due to stator indexing: the length of the separation bubble, the production of turbulence and the strength of periodic fluctuations downstream of the clocked stator.

In the following, the influences of stator clocking on performance and flow field of a 2.5-stage low-speed axial compressor using highly loaded CDA blade sections are investigated. Besides the stage characteristics for different clocking configurations, traverse data from pneumatic 5-hole probes and results from time-resolved unsteady total pressure measurements are used to gain a basic understanding of the flow mechanisms

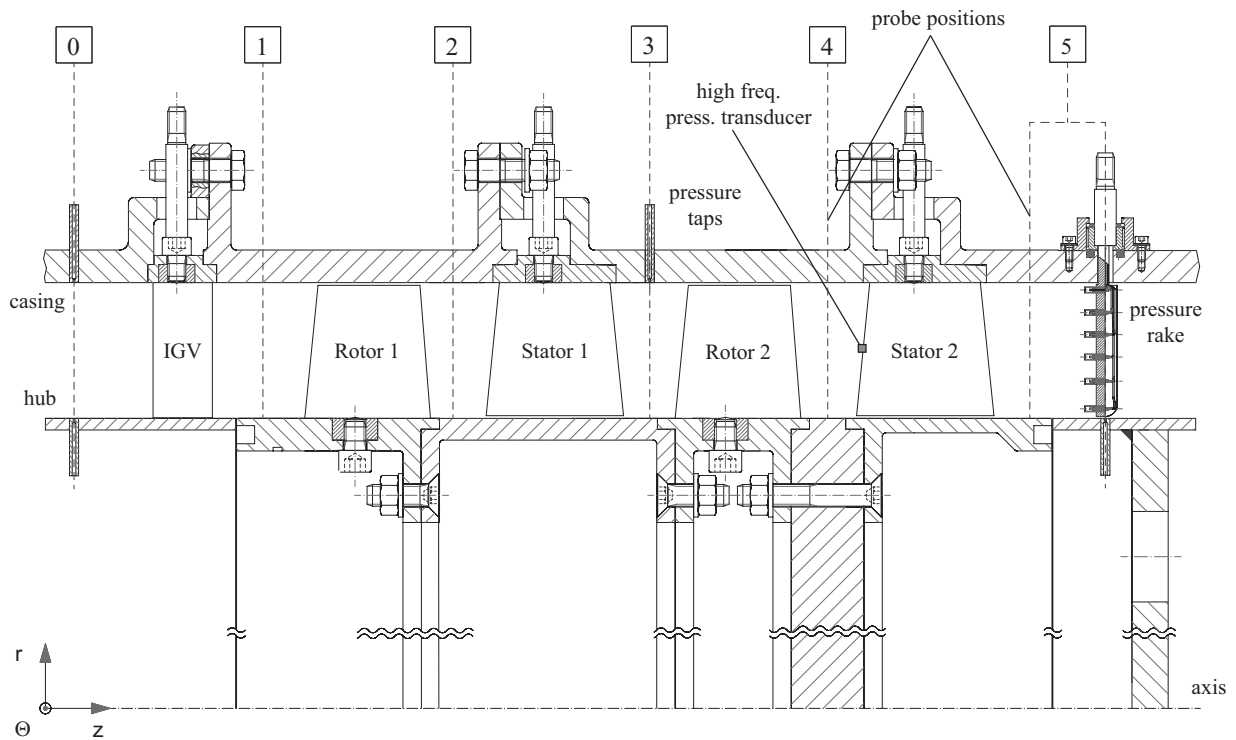


Figure 1. 2.5-STAGE LOW-SPEED RESEARCH COMPRESSOR

involved. Another crucial objective of this research was to keep the measurement uncertainty within acceptable limits. The present work is part of an in-depth survey on clocking effects in a low-speed axial compressor with the intent to gain improved knowledge of the related flow physics and interaction mechanisms. Additionally, the extensive experimental results provide a data basis for the validation of a numerical approach to complex multistage flows and wake-airfoil interactions.

Table 1. MAIN DESIGN PARAMETERS

Design parameters		
Flow coefficient:	$\varphi_D$	= 0.52
Pressure coefficient:	$\psi_{tt,D}$	> 1.6
Casing diameter:	$D_C$	= 0.6 m
Hub to tip ratio:	$v$	= 0.75
Aspect ratio:	$h/l$	= 1.0
Tip clearance to chord ratio:	$s/l$	= 0.01
Speed of rotation:	$n$	= 2800 rpm

## EXPERIMENTAL SETUP AND PROCEDURE

### Test Rig

The 2.5-stage low-speed research compressor (LSRC) consists of an inlet guide vane and two geometrically identical stages. Each stage contains a rotor row (43 blades) and a cantilevered stator row (45 vanes), utilizing front loaded CDA (Controlled Diffusion Airfoil) blade sections. A detailed description of the single-stage setup of the LSRC, which is identical in construction to the two-stage build, is given by Rohkamm et al. [13]. The experimental setup is shown in Fig. 1. Pressure taps for static pressure measurements are located in planes 0 to 5, while total pressure is determined via a pressure rake downstream of Stator 2. 5-hole probes can be installed in all six measuring planes. The LSRC is driven by a DC swivel bearing motor in order to ensure a precise adjustment of rotational speed and an accurate calculation of compressor power by measuring the reaction torque. To maintain a constant aerospeed during test runs, the DC motor is regulated via a closed-loop control system.

The main design parameters of the compressor stage, designed by Gümmer et al. [14] are shown in Table 1. The Reynolds number based on chord length and relative inlet velocity at the rotor tip is  $Re \approx 5 \cdot 10^5$  for design flow conditions. As the Mach number does not exceed  $Ma = 0.26$  anywhere in the compressor flow field, the flow can be considered incompressible.

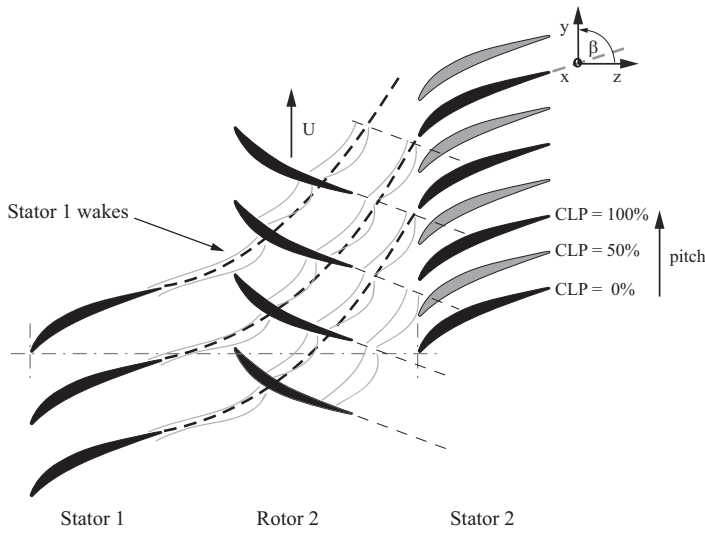


Figure 2. DEFINITION OF THE CLOCKING POSITION

### Stator Indexing

Due to the segmental test rig design philosophy, it is possible to rotate all three stator rows, including the IGW, independently up to one and a half stator pitches (i.e.  $12^\circ$ ) via remote controlled stepper motors. By this means, the relative circumferential positions of both stators and the IGW can be varied by increments of less than  $0.1^\circ$ . For the clocking investigations different indexing configurations were set by moving Stator 2 in rotational direction to a designated circumferential position (see Fig. 2). The relative positions of IGW and Stator 1 were unchanged, which localizes the clocking effect in the second stator row. The reference clocking angle, i.e. a CLP of  $0^\circ$  (0% Stator 2 pitch), applies, if Stators 1 and 2 are geometrically congruent in axial direction. Concerning the overall performance analysis, 17 clocking positions in  $0.5^\circ$  (i.d. 6.25%) pitches will be considered, with CLPs 0% and 100% providing identical vane positions. 5-hole probe area traverses were accomplished by turning all three stator rows in unison, thus accounting for the stationary nature of the probes and maintaining the clocking position of Stator 2.

### Compressor Characteristics

The overall static pressure ratio  $\Pi_{ss}/\Pi_{ss,D}$  was evaluated using pressure taps at hub and casing about one chord upstream of the IGW and one chord downstream of Stator 2. To determine the total-to-total pressure ratio  $\Pi_{tt}/\Pi_{tt,D}$ , total pressure data were collected via a pressure rake installed in plane 5 (see Fig. 1). Since the rake was traversed incrementally over a stator pitch, total pressure measurements were found to be rather time-consuming. Therefore, the number of measuring cycles per measuring point had to be kept relatively low. This amplified the

measuring uncertainty to such an extent that total pressure data became an inadequate means to identify the rather small impact of airfoil clocking on compressor performance. However, a sufficient number of measurement cycles ( $j = 160$ ) could be realized for the measurements of the static-to-static characteristics. Thus, the specific work which is done on the compressor mass flow  $\dot{m}$  shall be defined in terms of the static-to-static formulation between planes 0 and 5 in Fig. 1.

$$Y_{ss} = \frac{\gamma}{\gamma-1} R T_0 \left[ \left( \frac{p_5}{p_0} \right)^{\frac{\gamma-1}{\gamma}} - 1 \right] \quad (1)$$

The inner specific work is determined by the shaft speed and the torque and is again based on the mass flow rate.

$$Y_i = \frac{2 \pi n M}{\dot{m}} \quad (2)$$

With the given specific works the static-to-static compressor efficiency yields to:

$$\eta_{ss} = \frac{Y_{ss}}{Y_i} \quad (3)$$

The measurement uncertainty of the efficiency data due to dispersion about the mean was determined experimentally. It depends on the operating point and does not exceed  $\pm 0.05\%$  when testing data are arithmetically averaged over 160 measurement cycles. It is of interest to note, that all measurements were conducted after at least one hour of warm-up running time, which is sufficient to achieve a steady compressor operation. In an effort to prevent potential drift in the pressure transducers, they were re-zeroed prior to each test.

All compressor characteristics presented are normalized by the stage design parameters. All quantities were corrected to ISA sea level conditions. The LSRC static-to-static performance map for the reference clocking position is given in Fig. 3. The operation points that were investigated preferentially are referenced.

### Traverse Measurements

Two calibrated pneumatic 5-hole probes were used to conduct Stator 2 inlet and exit traverses to derive contour plots of the velocity and the mass-averaged total pressure distributions in planes 4 and 5 (see Fig. 1). The probe was traversed in radial direction from 5% to 95% annulus height in steps of 5% span. The resolution in pitchwise direction was  $0.25^\circ$ , which led to 33 circumferential times 19 radial measuring points per area

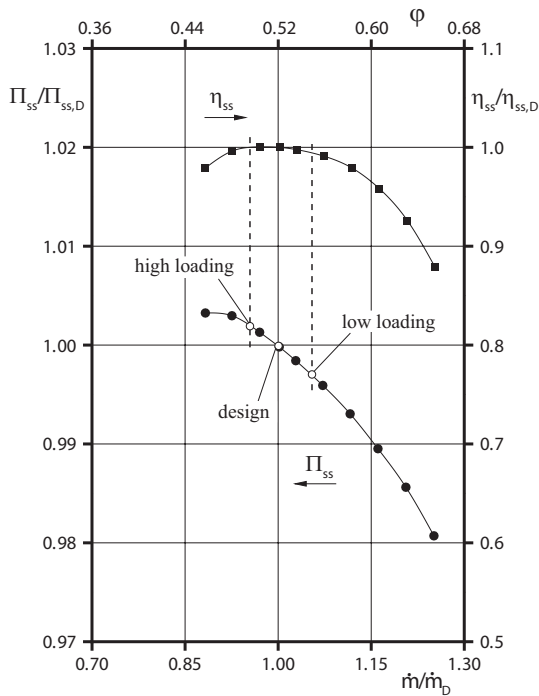


Figure 3. OVERALL LSRC PERFORMANCE AT DESIGN SPEED

traverse. To obtain more detailed information on the loss production of the clocked stator row additional 5-hole probe data were collected for three different spanwise positions (25%, 50% and 75% blade height) upstream and downstream of Stator 2. For the measurements, the quarter of the blade pitch which encompassed the Stator 2 wake was segmented into circumferential increments of 1.25% pitch ( $0.1^\circ$ ). Apart from that, the flow quantities were recorded in 3.125% pitch ( $0.25^\circ$ ) steps, which resulted in a total of 45 measuring points pitch-wise. Given that the exact streamline propagation from plane 4 to 5 was unknown, the mass-averaged Stator 2 loss coefficient had to be derived from circumferentially averaged inflow data. It is defined as:

$$\zeta_{S2} = \left\langle \frac{\langle p_{t4} \rangle - p_{t5}}{Q_4} \right\rangle \quad (4)$$

All traverse measurement data were corrected to ISA sea level conditions.

### Unsteady Total Pressure Measurements

Information on the Stator 1 wake propagation based on the Stator 2 clocking position was obtained using a high frequency response piezoresistive pressure transducer (Endevco 8507C-1) embedded in a single Stator 2 blade. Unsteady total pressure measurements were carried out at midspan about 1mm upstream

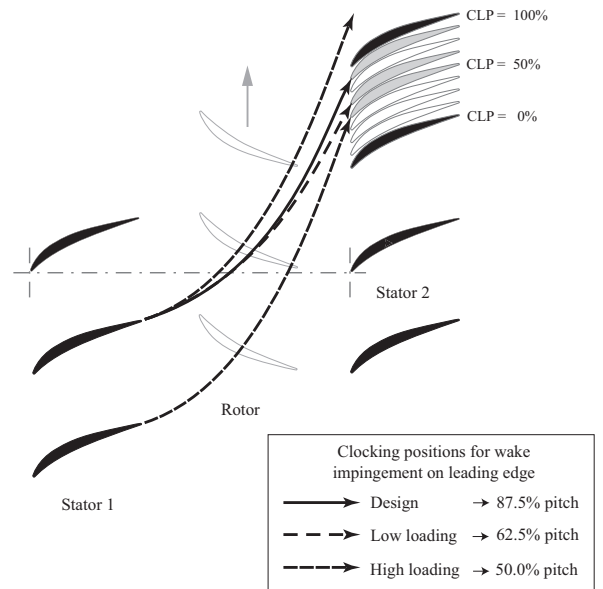


Figure 4. STATOR 1 WAKE TRAJECTORIES

of the leading edge to locate the upstream stator wake path in relation to the clocked stator (see Fig. 2). A once per revolution TTL trigger signal allowed ensemble averaging of the measured raw time signal which consisted of 256 ensembles, each with 1024 measuring points around the circumference. The sampling frequency was set to approximately 48.5kHz and a low pass filter of 21.4kHz was applied. The ensemble and time averaging techniques used for this paper are given by König et al. [11].

Please note that the applied sensor did not account for deviations from design inflow incidence. Hence, the measured total pressure may vary from the actual absolute value at low and high loading conditions. However, this effect has proven to be negligible as far as the detection of the Stator 1 wake is concerned.

## RESULTS

### Clocking Effects on Global Performance

Given that during previous investigations the clocking effect was usually found to depend on the compressor operating point, performance analyses were conducted basically for three different blade loading conditions. These were design, low and high loading, i.e.  $\dot{m}/\dot{m}_D = 1.0$ , 1.056 and 0.953, respectively. Additional performance data were acquired at near stall condition,  $\dot{m}/\dot{m}_D = 0.88$ , and for very low blade loading at  $\dot{m}/\dot{m}_D = 1.1$  and 1.173. To attain repeatable performance data, the mass flow was held constant during testing procedure and measurements were taken every 6.25% of Stator 2 pitch starting at the reference CLP of 0%. In order to exclude a potential measurement hysteresis caused by the indexing process and to ascertain

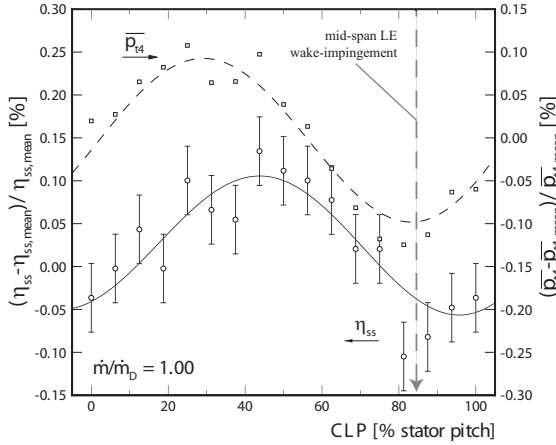


Figure 5. CLOCKING EFFECT ON  $\eta_{ss}$  AND  $p_{t4,ms}$ :  $\dot{m}/\dot{m}_D = 1.00$

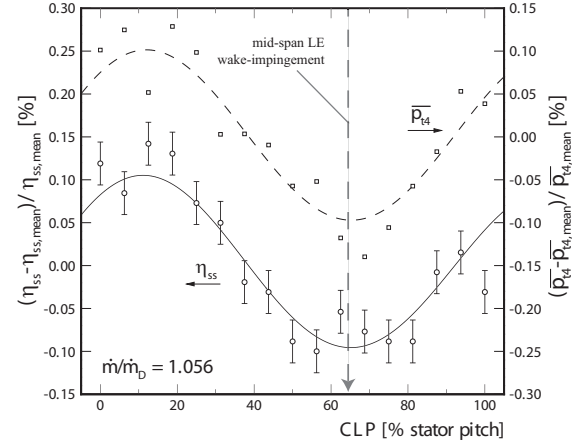


Figure 6. CLOCKING EFFECT ON  $\eta_{ss}$  AND  $p_{t4,ms}$ :  $\dot{m}/\dot{m}_D = 1.056$

repeatability, performance tests were repeated at least twice and also in reversed clocking direction.

The propagation of the Stator 1 wake through the second stator row was identified via a high-frequency response piezoresistive pressure transducer applied in a single Stator 2 blade at mid-span. Similarly to compressor efficiency time-resolved total pressure data were collected just upstream of Stator 2 leading edge for corresponding clocking positions. Here, a minimum in time-averaged total pressure indicates a Stator 1 wake impingement directly onto the Stator 2 leading edge at mid-span, whereas a maximum locates the wake trajectory through mid-passage. It is of interest to note, that the Stator 1 wake measured in this manner does not always originate from the same stator vane. Fig. 4 presents a schematic of the Stator 1 wake trajectories and highlights their dependence on operation condition. Although not shown here, the wake propagation measurements were verified by means of 5-hole probe measurements upstream of Stator 2.

Figs. 5, 6 and 7 show the results of the LSRC global performance measurements as variations from the mean value over the Stator 2 clocking position for the operating conditions  $\dot{m}/\dot{m}_D = 1.0$ , 1.056 and 0.953, respectively. Included are the accompanying time-averaged total pressure quantities displayed in a uniform manner. Approximation curves help to illustrate both clocking-related trends. It is shown that variations in overall compressor efficiency due to Stator 2 indexing are minor but clearly exceed measurement uncertainty and are exhibiting an almost sinusoidal trend over the clocking angle. The potential of stator clocking for all three operating points is around 0.2% of mean global LSRC efficiency.

For design and low loading conditions variations in total pressure and compressor performance due to airfoil clocking are of the same order. Regarding the higher flow coefficient, the total

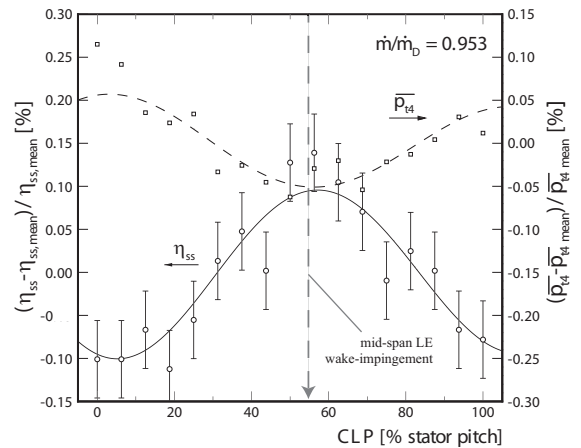


Figure 7. CLOCKING EFFECT ON  $\eta_{ss}$  AND  $p_{t4,ms}$ :  $\dot{m}/\dot{m}_D = 0.953$

pressure measurements suggest best overall performances, if the Stator 1 wakes pass through mid-passage of Stator 2 (Fig. 6). In this case, the pressure and efficiency peaks coincide at optimum clocking positions of about 12.5% stator pitch. A performance minimum occurs at a clocking configuration where the Stator 1 wakes impinge on the downstream stator row leading edges at 50% span. Similar observations can be made for design loading with only a slight offset of less than 10% stator pitch clockwise between the best efficiency CLP (43.75% stator pitch) and the captured total pressure peak. Due to the sinusoidal nature of the efficiency distributions the respective extremes of both operation conditions are offset by half a stator pitch from one

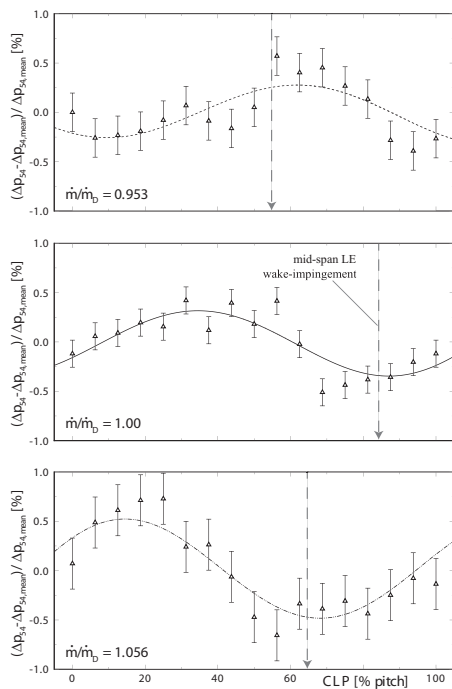


Figure 8. CLOCKING EFFECT ON STATOR 2 PERFORMANCE

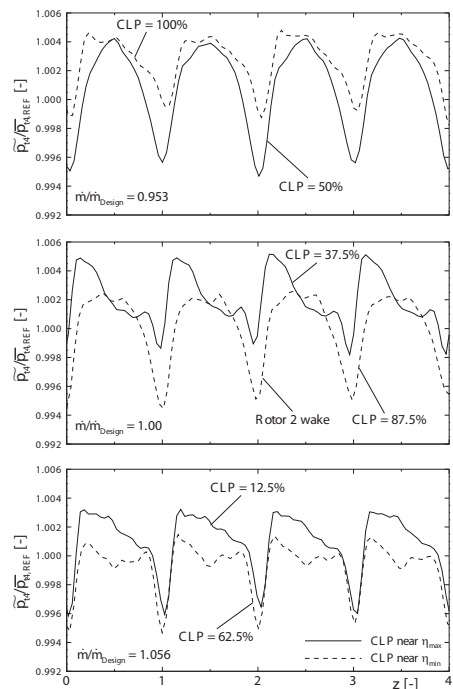


Figure 9. ENSEMBLE-AVERAGED TOTAL PRESSURE

another. Although a further decrease in blade loading indicates similar tendencies as those mentioned above, a reduced clocking potential in conjunction with an increased measurement uncertainty prevents a reliable verification of the vane clocking effect at higher flow coefficients (not shown here). The increase in measurement uncertainty is basically due to the steeper slope of the pressure rise characteristic at higher flow coefficients (see Fig. 3), where a small fluctuation in flow will result in a much larger offset from mean pressure rise than for the higher loaded operation conditions. As opposed to the results at design and low loading the clocking configuration providing leading edge impingement of the upstream stator wake appears to be the optimum efficiency condition at high loading (Fig. 7). A maximum can be found at a CLP of about 50% pitch. Otherwise, the Stator 1 wake path propagating through Stator 2 mid-passage, which is indicated by a peak in time-averaged total pressure, results in worst compressor performance at reference CLP. However, total pressure measurements at the Stator 2 leading edge prove, that an increase in loading results in a more shallow and less defined Stator 1 wake. In fact, this leads to a negligible clocking potential at near stall conditions (not shown here). As far as the indexing positions for highest and lowest efficiency are concerned, the present work only accords with Barankiewicz & Hathaway [1] who also investigated stator clocking in a low-speed environment. Interestingly, it directly opposes most clocking analyses using medium- or high-speed compressors, like Key et al. [2].

Please note, that due to minor temperature changes along the compressor axis it is not feasible to calculate LSRC efficiency via temperature rise. Thus, the separation of stage efficiency from overall efficiency is impossible. In order to isolate and evaluate the effects of clocking on the clocked blade row, Fig. 8 presents the variations in normalized Stator 2 pressure rise from the mean value as a function of CLP at the three surveyed operating conditions. The quantities were derived from pressure tap measurements in compressor planes 4 and 5 and made non-dimensional via the corresponding mean static pressure rise across Stator 2. The given results are consistent with the trends of overall compressor efficiency, including clocking positions for maximum and minimum performance. Regarding the potential of stator clocking on Stator 2 pressure rise, variations as high as 1% for design and high loading and 1.4% for low loading were observed. Again, the effects of clocking exceed measuring uncertainty.

Looking at the ensemble averaged total pressure acquired at the Stator 2 inlet by means of a high frequency response piezoresistive pressure transducer, the crucial impact of stator clocking on the unsteady Stator 2 inflow becomes evident. Fig. 9 shows plots of the ensemble averaged time-resolved total pressure signals about 1mm upstream of the Stator 2 leading edge at mid-span featuring optimum (solid line) and worst case (dashed line) indexing positions for three operating conditions. The displayed time span is 4 rotor blade passings, i.e. 9.3% of one rotor revolution. Signals are normalized with the respective time

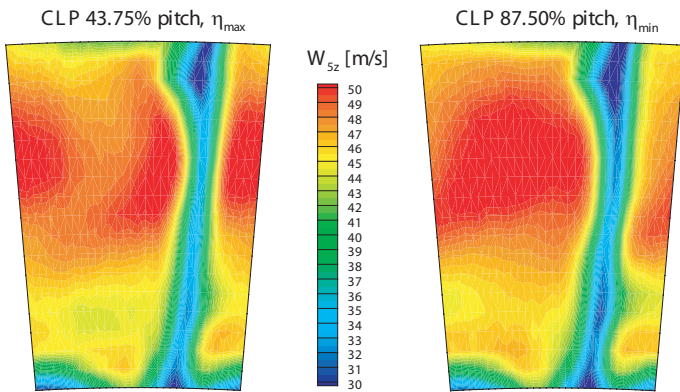


Figure 10. STATOR 2 EXIT AXIAL VELOCITY:  $\dot{m}/\dot{m}_D = 1.00$

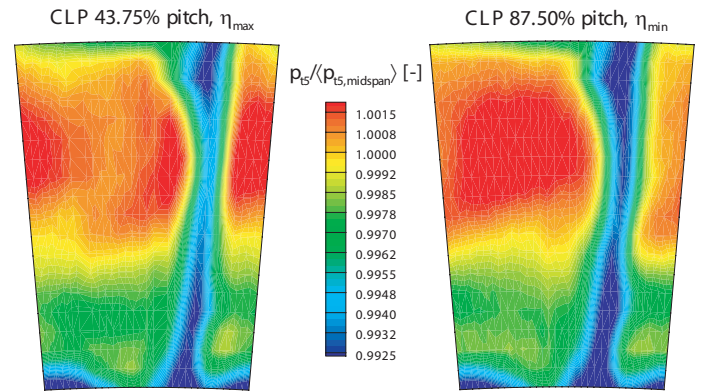


Figure 11. STATOR 2 EXIT AXIAL TOTAL PRESSURE:  $\dot{m}/\dot{m}_D = 1.00$

averaged total pressure value of the reference clocking configuration for the given operating point. It is observed, that Stator 1 wake impingement considerably lowers the measured total pressure which can be seen in a strengthening of the periodic Rotor 2 wakes and the creation of an intermediate pressure plateau. Concerning the coherence of best efficiency and wake impingement, the displayed trends are images of the time-averaged results and appear well-defined for low and high loading. Design loading, however, shows a minor overlap of the time-resolved total pressure distributions for minimum and maximum efficiency which may result from compressor performance being slightly out-of-phase with the time-averaged total pressure at this operating condition. The fact, that not two of the inflow patterns look alike, indicates the complex nature of the flow field and its sensitivity to different Stator 2 circumferential positions.

### Contour Plots

Figs. 10 and 11 show the time-averaged results of the finely resolved Stator 2 exit traverses. Given are the contour plots of velocity (Fig. 10) and mas-averaged total pressure (Fig. 11) distributions in plane 5 for optimum and worst case clocking positions at design loading. Passages were measured from 0% to 100% Stator 2 pitch and from 5% to 95% span. The total pressure was normalized with the respective pitch-averaged quantity at mid-span. The data were obtained by employing a calibrated 5-hole-probe downstream of Stator 2 and traversing the IGV and both stators in unison past the probe, while keeping the CLP fixed.

For both clocking positions the Stator 2 wake is clearly defined by the straight and narrow region of velocity and total pressure defects, respectively. Considering the differences between both configurations, it is observed that Stator 2 indexing leads to a circumferential redistribution of the flow. The Stator 1 wake can be identified only for the 43.75% pitch CLP for best performance as a bow-shaped low-velocity disturbance in the

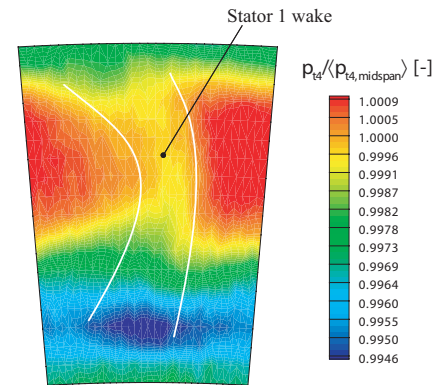


Figure 12. ROTOR 2 EXIT AXIAL TOTAL PRESSURE:  $\dot{m}/\dot{m}_D = 1.00$

otherwise high-velocity mid-passage region for the majority of the span. With a CLP of 87.5% pitch, signifying a performance minimum, Stator 2 and Stator 1 wakes coalesce for the most part. This results in a significantly wider and deeper Stator 2 wake region over the entire span as compared to the best efficiency case, while the mid-passage flow remains undisturbed. The considerable span-wise skewness of the Stator 1 wake is confirmed in Fig. 12. It shows the Rotor 2 exit flow in a mass-averaged total pressure contour plot including the Stator 1 wake residue, which is highlighted to allow a convenient localization. Note, that the Rotor 2 exit flow remains unaffected by the clocking of Stator 2 and therefore is not assigned to a specific CLP. Consequentially to the bow-like shape of the Stator 1 wake, the aerodynamic clocking position for Stator 2 may vary slightly from hub to tip. However, from about 50% to 70% span the wake-skew is less distinctive and the aerodynamical clocking position can be considered consistent.

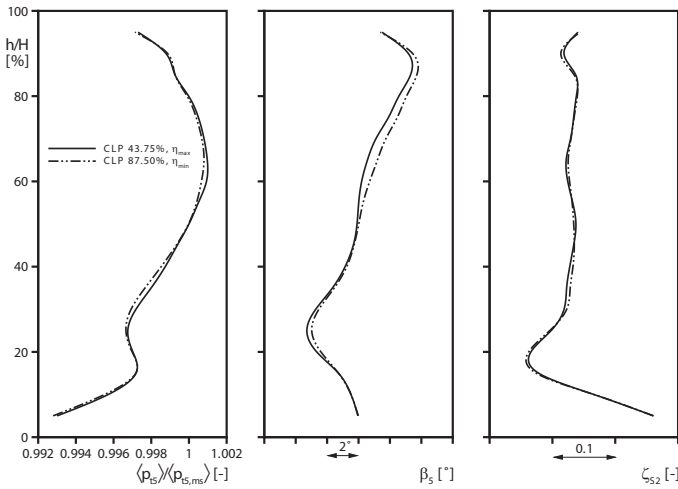


Figure 13. STATOR 2 EXIT FLOW PARAMETERS:  $\dot{m}/\dot{m}_D = 1.00$

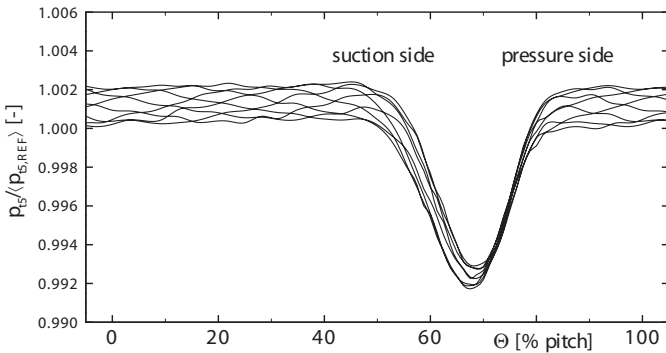


Figure 14. STATOR 2 TOTAL PRESSURE:  $\dot{m}/\dot{m}_D = 1.00$ ,  $h/H = 75\%$

### Radial Distributions

The circumferentially averaged radial distributions of total pressure, Stator 2 outflow angle and loss coefficient are presented in Fig. 13. The data was derived from the high-resolution 5-hole probe traverses in measuring plane 5 with additional measurements conducted downstream of Rotor 2 for the loss coefficient calculation. Thus, the investigated clocking positions are also for best and worst case compressor performance at design operation condition. The total pressure radial profiles were normalized with the pitch-averaged value of the maximum efficiency configuration at mid-span.

The total pressure distributions line up nearly identical for both extreme efficiency conditions. However, at spans around 25%–40% and 50%–70% the best performance CLP exhibits small advantages in total pressure rise. The radial Stator 2 outflow angle profiles give a possible explanation. For a major part of the span, particularly in a region where the skew of the

incoming Stator 1 wake is negligible (see Fig. 12), the integral outflow angle is increased about more than  $1^\circ$  if the Stator 1 wake path is positioned on the Stator 2 leading edge. A higher stator outflow angle may indicate a stronger deviation of the flow, which by trend leads to a lower pressure rise. Presumably due to the small scale variations being lost to measurement uncertainty, this tendency cannot be observed in the Stator 2 loss coefficient profiles. A span-wise integration of Stator 2 loss coefficients suggests higher losses for the minimum efficiency clocking position, nevertheless.

### Circumferential Profiles at Different Spans

While probe traverses of such fine resolution are justified in order to pinpoint the variation of the flow field and the impact of clocking, the procedure is very time-consuming. Therefore, further investigations on this matter will isolate Stator 2 spans of 25%, 50% and 75%, each surveyed at eight clocking positions, that are spread uniformly across the Stator pitch, to detect peaks in local performance.

To give an impression of the sensitivity of Stator 2 flow to the stators circumferential position Fig. 14 shows the non-dimensional total pressure distributions for eight CLPs in measuring plane 5 at design LSRC operation and 75% span. The total pressure profiles are aligned in circumferential position and are normalized with the respective pitch-averaged value of the reference clocking position. Additionally, the suction- and pressure-sided regions of the Stator 2 wake have been marked accordingly. The variations associated with stator clocking occur in the freestream total pressure as well as in the Stator 2 wake thickness and depth. Local variations are found to be dependent on span and blade loading. They can be as high as 15% of the Stator 2 pressure rise in the freestream region and appear to be less developed at the wake low point. In accordance with previous studies on vane clocking, the impingement of the upstream stator wake primarily thickens and deepens the suction-sided part of the Stator 2 wake, while the pressure-sided wake region remains largely unaffected. This leads to the assumption that suction side boundary layer development and its response to wake impingement may play a decisive role on clocking effects. Figs. 15, 16, and 17 show the mass-averaged Stator 2 exit total pressure at 75%, 50% and 25% span for mass flows  $\dot{m}/\dot{m}_D = 1.0$ , 1.056 and 0.953, respectively. For each span, the clocking configurations for maximum and minimum overall compressor performance were aligned and compared.

Regarding design operation (Fig. 15), it becomes evident, that the impact of the Stator 1 wake on the leading edge of Stator 2 (at mid-span), which happens near 87.5% Stator 2 pitch, effects the considered spans differently. While 25% and 75% spans feature Stator 2 wakes, that are thickened and deepened considerably, the wakes at mid-span show little difference between best and minimum overall efficiency configurations.

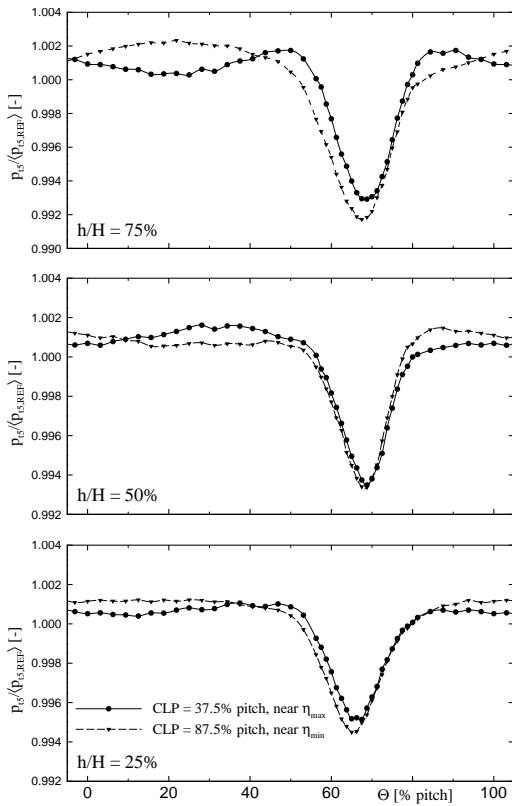


Figure 15. STATOR 2 EXIT TOTAL PRESSURE:  $\dot{m}/\dot{m}_D = 1.00$

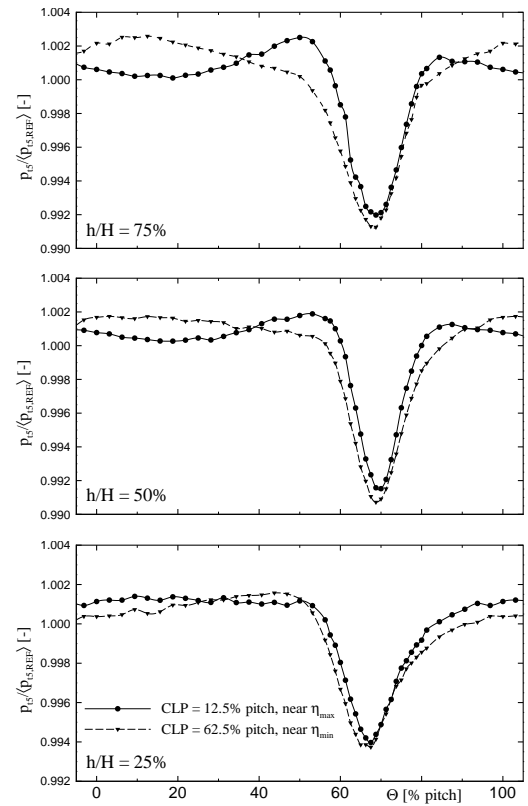


Figure 16. STATOR 2 EXIT TOTAL PRESSURE:  $\dot{m}/\dot{m}_D = 1.056$

Furthermore, the progression of the freestream area at mid-span appears to be flattened if the Stator 1 wake impinges at the leading edge, which stands in contrast to the flow at spans near hub and casing. The effects of stator clocking always occur in the suction-sided region of the wake, whereas the pressure sides of the wake usually align. This is true for all spans at design as well as low loading (Fig. 16), where the basic influences of clocking are unchanged. Here, a clocking position of 12.5% pitch delivers best compressor performance, whereas a CLP of 62.5% indicates the most disadvantageous configuration with Stator 1 wake impingement. The total pressure profiles for 50% and 75% span are almost identically in trend, showing the above mentioned effects very prominently. This may be based on the upper-span region of comparatively high axial velocities reaching well beyond mid-span at high flow coefficients in contrast to design operation (Fig. 10), where the 50% span marks a strong gradient in axial velocity from upper to lower span. As expected for the best efficiency case, both stator wakes are easily discernible from each other and do not coalesce. However, this does not completely apply at 25% span, where the position of the Stator 1 wake is shifted in negative pitch direction for both clocking positions, certainly as a consequence of the wake-skew effect. Otherwise, the variations due to Stator 2 indexing at 25% span and low blade loading are

not as distinctive as for the upper spans. The results of probe traverses at all three spans for high loading operation are presented in Fig. 17. Even though highest global efficiency at low flow coefficients was achieved for Stator 1 wake impingement (CLP = 50% pitch), the total pressure profiles in measurement plane 5 for this configuration feature a thinner and shallower Stator 2 wake and a somehow levelled freestream region, coinciding with the trend for maximum compressor efficiency at design and low loading. Again, this is only true for the distributions at 50% and 75% span. At 25% span, the Stator 2 wake remains mostly unaffected by clocking and variations can only be found in the freestream area.

A possible explanation for the different responses of Stator 2 to Stator 1 wake impingement is that the turbulence of the incoming wake should be helpful at high loading in suppressing separations, yet disadvantageous near design and higher flow coefficients because it will initiate early transition and thus thicken the suction side boundary layers. As to how the Stator 1 wake propagation through Stator 2 and its influence on boundary layer transition eventually result in the presented Stator 2 total pressure profiles cannot be entirely discerned from mere 2D-measurements and certainly deserves further study. Nevertheless it is demonstrated, that while the aerodynamic clocking position

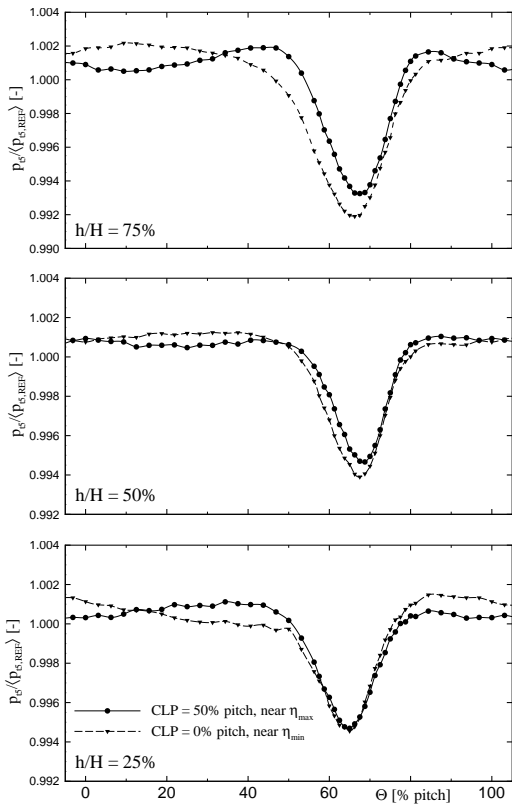


Figure 17. STATOR 2 EXIT TOTAL PRESSURE:  $\dot{m}/\dot{m}_D = 0.953$

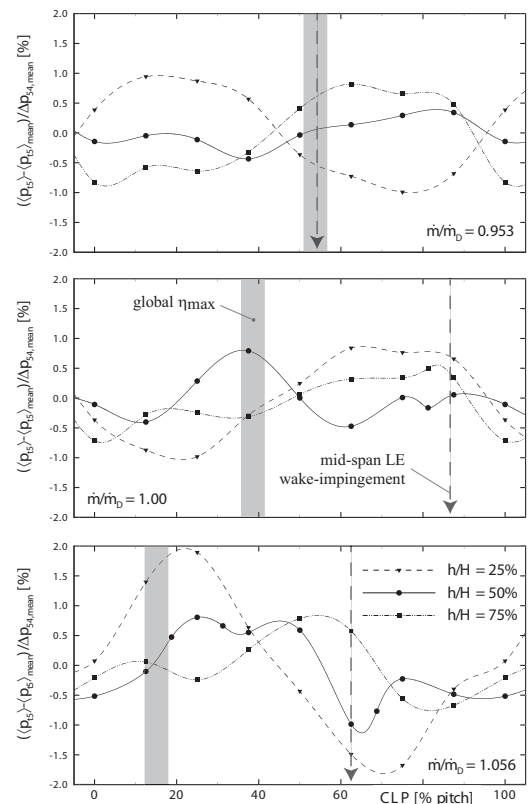


Figure 18. PITCH-AVERAGED STATOR 2 EXIT TOTAL PRESSURE

may vary from hub to casing to a certain degree, the clocking configuration that leads to a thinner and shallower Stator 2 wake will always be the one most beneficial to LSRC performance.

To identify extremes in local performance, the variations in pitch-integrated total pressures for 25%, 50% and 75% span and three operation points over the Stator 2 clocking position are presented in Fig. 18. The quantities are normalized with the mean Stator 2 static pressure rise. In addition, the clocking positions for leading edge wake-impingement and best overall compressor performance are highlighted, the latter via shaded bands with a width of about 6.25% stator pitch to take account for the inaccuracy in efficiency determination. Regarding the results of pitch-integrated total pressure variation downstream of Stator 2 at design operation, only the profile at 25% pitch appears to be roughly sinusoidal over the clocking angle. Unexpectedly, the 50% and 75% span distributions follow no noticeable trend. Despite the somewhat arbitrary spreading of measuring points, there is a distinct maximum in total pressure variation for 50% span of about +0.6% coinciding with the global efficiency peak. Interestingly, the quantities at 25% span seem to be out-of-phase as compared to the global trend. This is based on the fact that the local aerodynamic clocking position for maximum performance varies across the span. The results at low loading ( $\dot{m}/\dot{m}_D = 1.056$ )

resemble those at design operation, safe for the fact that this time the maxima and minima in variation of 25% span total pressure and global performance concur. The total pressure profiles at 50% and 75% span, again, feature no cognizable trend. For the high loading condition the Stator 2 exit total pressure variations at 25% and 75% follow near-sinusoidal trends, whereas the changes at mid-span are minor and more ambiguous in comparison. Again, the 25% and 75% span progressions are clearly out of phase with the 75% span local performance peak being closer to the global maximum.

While these results alone hardly allow any conclusion to be drawn on the exact nature of the effects of clocking, it could be verified that the Stator 2 spans react differently to a given clocking position. This effect certainly weakens the advantages of airfoil clocking on a global scale, as local performance maxima of benefited spans may get compensated by an unfavourable reaction to the same CLP elsewhere on the blade. How the clocked stator will respond to a given clocking position on the whole will most likely depend on where the majority of the flow runs through the annulus. At least for design and high loading this is in the upper half of the span. Hence, the influences of the 50% and 75% spans will predominantly dictate the global tendency for these operation points, as shown in in Fig. 18.

## CONCLUSIONS

The effects of stator clocking on performance and flow field of a 2.5-stage low-speed axial compressor utilizing front loaded CDA blade sections have been studied. Experimental investigations for different Stator 2 clocking positions at design, low and high loading conditions and design speed were conducted including measurements of stage performance and unsteady total pressure at the Stator 2 leading edge as well as 5-hole probe traverse measurements. The following conclusions have been drawn:

i) The potential of stator clocking for all three operating points is approximately 0.2% in global efficiency. Regarding the static pressure rise across the clocked stator row, the variations due to clocking were found to be as high as 0.9% for high and design loading and 1.4% for low loading.

ii) For design and low loading conditions best overall performance is achieved, if the Stator 1 wakes pass exactly through mid-passage of Stator 2, whereas at high loading maximum efficiency places the wake trajectory directly at the leading edge. In this point the present survey (compressor) significantly differs from most previous clocking studies carried out in higher speed environments.

iii) Stator Clocking influences the thickness of the Stator 2 suction side wake profile considerably. The clocking configuration that leads to a thinner and shallower Stator 2 wake is most beneficial to compressor performance for any operation condition.

iv) A span-wise skewness of the upstream stator wake leads to a moderate variation of the aerodynamic clocking position across the Stator 2 span. This effect eventually weakens the advantages of airfoil clocking on a global scale.

v) In order to get complete understanding of the flow physics related to clocking and to be able to introduce them into the design process, an investigation of the unsteady boundary layer behaviour of the clocked stator row will prove helpful.

## ACKNOWLEDGEMENT

This research was funded within the frame of the German LuFo IV program VerDeMod 20T0609. The authors would like to thank Rolls-Royce Deutschland Ltd Co KG for encouraging and approving the publication of this work.

## REFERENCES

- [1] Barankiewicz, W.; Hathaway, M., 1997. *Effects of Stator Indexing on Performance in a Low Speed Multistage Axial Compressor.*, ASME Gas Turbine Conference and Exposition, Paper 97-GT-496.
- [2] Key, N.; Lawless, P.; Fleeter, S., 2008. *An Experimental Study of Vane Clocking Effects on Embedded Compressor Stage Performance.*, ASME Gas Turbine Conference and Exposition, Paper GT2008-51087.
- [3] Key, N.; Lawless, P.; Fleeter, S., 2008. *An Investigation of the Flow Physics of Vane Clocking Using Unsteady Flow Measurements.*, ASME Gas Turbine Conference and Exposition, Paper GT2008-51091.
- [4] Huang, H.; Yang, H.; Feng, G.; Wang, Z., 2003. *Fully Clocking Effect in a Two-Stage Compressor.*, ASME Gas Turbine Conference and Exposition, Paper GT2003-38867.
- [5] Saren, V.; Savin, N.; Dorney, D.; Sondak, D., 1998. *Experimental and Numerical Investigation of Airfoil Clocking and Inter-Blade-Row Gap Effects on Axial Compressor Performance.*, AIAA(Paper 98-3413), pp. 1 18.
- [6] Layachi, M.; Bölcş, A., 2001. *Effect of the Axial Spacing between Rotor and Stator with Regard to the Indexing in an Axial Compressor.*, ASME Gas Turbine Conference and Exposition, Paper 2001-GT-0592.
- [7] Huang, H.; Yang, H.; Feng, G.; Wang, Z., 2004. *Clocking Effect in a Two-Stage Compressor with Different Inter-Blade-Row Gaps.*, Journal of Thermal Science, 13(1), pp. 8 15.
- [8] He, L.; Wells, R.; Li, Y.; Ning, W., 2002. *Analysis of Rotor-Rotor and Stator-Stator Interferences in Multi-Stage Turbomachines.*, Journal of Turbomachinery, 124(4), pp. 564 571.
- [9] Walker, G.; Hughes, J.; Solomon, W., 1999. *Periodic Transition on an Axial Compressor Stator: Incidence and Clocking Effects: Part I – Experimental Data.*, Journal of Turbomachinery, 121, pp. 398 407.
- [10] Solomon, W.; Walker, G.; Hughes, J., 1999. *Periodic Transition on an Axial Compressor Stator: Incidence and Clocking Effects: Part II – Transition Onset Prediction.*, Journal of Turbomachinery, 121, pp. 408 415.
- [11] König, S.; Stoffel, B.; Taher Schobeiri, M., 2009. *Experimental investigation of the Clocking Effect in a 1.5-Stage Axial Turbine – Part I: Time-Averaged Results.*, Journal of Turbomachinery, 131(2), 021003.
- [12] König, S.; Stoffel, B.; Taher Schobeiri, M., 2009. *Experimental investigation of the Clocking Effect in a 1.5-Stage Axial Turbine – Part II: Unsteady Results and Boundary Layer Behaviour.*, Journal of Turbomachinery, 131(2), 021004.
- [13] Rohkamm, H.; Wulff, D.; Kosyna, G.; Saathoff, H.; Stark, U.; Gümmer, V.; Swoboda, M.; Goller, M., 2003. *The Impact of Rotor Tip Sweep on the Three-Dimensional Flow in a Highly-Loaded Single-Stage Low-Speed Axial Compressor: Part II – Test Facility and Experimental Results.*, Proceedings of the ETC 5, pp. 175-185.
- [14] Gümmer, V.; Swoboda, M.; Goller, M.; Dobat, A., 2003. *The Impact of Rotor Tip Sweep on the Three-Dimensional Flow in a Highly-Loaded Single-Stage Low-Speed Axial Compressor: Part I – Design and Numerical Analysis.*, Proceedings of the ETC 5, pp. 163-174.